Fatigue performance enhancement of selectively laser melted aluminium alloy by heat treatment

I. Maskery,[1, *] N.T. Aboulkhair,[2] C. Tuck,[1] R.D. Wildman,[1]
I.A. Ashcroft,[1] N.M. Everitt,[2] and R.J.M. Hague[1]

*[1]Manufacturing and Process Technologies Research Division,
Faculty of Engineering, University of Nottingham, Nottingham NG7 2RD, UK*
*[2]Materials, Mechanics and Structures Research Division,
Faculty of Engineering, University of Nottingham, Nottingham NG7 2RD, UK*

We measured the stress-strain behaviour and fatigue performance of the aluminium alloy Al-Si10-Mg manufactured by selective laser melting (SLM). This process, specifically the rapid cooling of the metal from its molten state, results in a fine microstructure, generally providing high hardness but poor ductility. We used a heat treatment to alter the microstructure of the material from its as-built state. This significantly improved the ductility and fatigue performance. The elongation at break for the heat treated material was nearly three times greater than that observed for the as-built material, and the fatigue strength at 10^6 cycles was around 1.6 times as high. Combined with the design freedoms of additive manufacture, this development increases the suitability of lightweight SLM parts for use in the aerospace and automotive sectors, where good fatigue performance is essential.

I. INTRODUCTION

Selective laser melting (SLM) is an additive manufacturing (AM) process that constructs parts through the repeated deposition and melting of metal powder layers. Because of this layerwise construction, SLM allows parts with very complex geometries to be made, including those that come from topology optimisation (TO) algorithms[1–4] or include lattice structures of tessellating cells[5–13]. Complex, weight minimising geometries can be manufactured with no additional expense, and often considerably reduced processing time, than more traditional forms, i.e. those designed for conventional processes such as casting or milling. Lattices also have the potential to provide high levels of energy absorption under static and dynamic loading and, compared to TO methods, may offer more robust solutions to problems which include uncertainty in the loading conditions or have multiple objectives. These features make SLM parts particularly well suited to the automotive and aerospace sectors, where the minimisation of component weight is a strong and persistent requirement.

For TO and lattice structures to be used effectively, and for the SLM process to be adopted into the relevant manufacturing sectors, the properties of SLM materials must be well understood. Authors have examined many properties of SLM materials[14–21], but there exists only a handful of investigations into their fatigue performance[22–27]. Of these, only Siddique *et al.*[22] and Brandl *et al.*[25] have investigated the fatigue performance of SLM Al-Si alloys, and only Brandl *et al.* have examined Al-Si10-Mg in particular.

---

*email: ian.maskery@nottingham.ac.uk

Siddique *et al.* investigated Al-Si12, focussing on the effects of laser energy density, base plate temperature, and a post-build stress relief on the mechanical properties. Brandl *et al.* examined Al-Si10-Mg, likewise looking at the effects of base plate temperature and a post-build heat treatment, in their case a T6 treatment which is often used to harden and strengthen conventionally produced Al-Si alloys. A few key findings of Siddique *et al.* and Brandl *et al.* are provided in section III of this work, where they are discussed in relation to our results. It is worth noting that in both of these previous investigations the SLM fatigue specimens were subject to mechanical finishing to reduce their surface roughness prior to testing. To provide results more representative of as-manufactured SLM parts, our specimens were tested with their relatively rough surfaces intact.

Heat treatments have been shown to significantly alter the microstructure and hardness of SLM Al-Si10-Mg[16]. This material, with an inherently fine microstructure arising from the SLM manufacturing process, responds differently to T6 or 'precipitation hardening' heat treatments than when it is conventionally processed. In the as-built condition, the microstructure is characterised by fine α-Al grains with Si continuously segregated at the grain boundaries. This material has a hardness of 109.9 $\pm$ 0.9 HV[16], which is high compared to the 86 HV of conventional cast and aged Al-Si alloy[14], but it is also relatively brittle (as seen in the stress-strain behaviour in section III). Enhancing the ductility of the material, by coarsening its microstructure with a post-manufacture heat treatment, could potentially increase the fatigue strength.

The main aim of this investigation is to determine how a T6-like heat treatment affects the microstructure, stress-strain behaviour and fatigue performance of SLM Al-Si10-Mg. Determining the relationship between these properties will add to the understanding of the material, and will support the development of effective post-manufacture processes for improving the mechanical performance of SLM alloys.

II. EXPERIMENTAL DETAILS

A. Selective laser melting of test specimens

A series of Al-Si10-Mg tensile test specimens and fatigue specimens were produced using a Renishaw AM250 SLM machine. The tensile tests were conducted using dog bone specimens in accordance with ASTM standard E8/E8M[28]. Their gauge length and diameter were 45 mm and 9 mm, respectively. The fatigue specimens had circular cross section and their geometry corresponded to ASTM standard E466-07[29]; the dimensions are shown in figure 1 and a photograph of a manufactured specimen is provided in figure 2. Both types of specimen were manufactured with their long axis perpendicular to the plane of the SLM build platform.

During SLM specimen production, the laser power was 200 W and the powder was deposited in 25 μm layers prior to each laser scan. The build platform was held at 180 °C throughout the manufacturing process. The laser rastered across the parts with a hatch spacing of 130 μm, a point distance of 80 μm and an exposure time of 140 μs, providing an effective scanning speed of 571 mm s^{-1}. The hatch direction of each layer was rotated by 67° from the previous one. Focused at the powder bed, the laser had a circular spot of
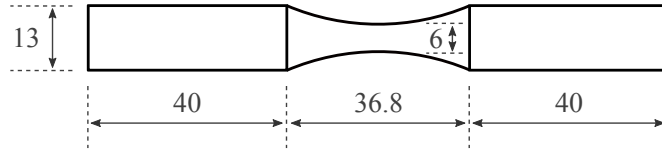
FIG. 1: Dimensions (in mm) of the fatigue specimens used in this work.

FIG. 2: SLM Al-Si10-Mg fatigue specimen. Note the additional 2 mm of supporting material at the specimen base, which was included to facilitate removal of the specimens from the SLM build platform.

diameter (68 ± 2) μm.

B. Heat treatment

The SLM Al-Si1-Mg specimens were tested in two conditions; as-built and heat treated. The post-manufacture heat treatment comprised a solution treatment for 1 hour at 520 °C followed by a water quench and artificial ageing for 6 hours at 160 °C. This treatment was found by Aboulkhair *et al.*[16] to modify the microstructure of SLM Al-Si10-Mg and reduce the hardness by nearly 30% from the as-built condition. This softening is in stark contrast to the effect on conventionally produced material, where treatments of this kind result in hardening through the precipitation of β-Mg$_2$Si particles.

The effect of the heat treatment on the SLM Al-Si10-Mg microstructure is shown in figure 3. The as-built material, with its characteristic melt pools and fine microstructure
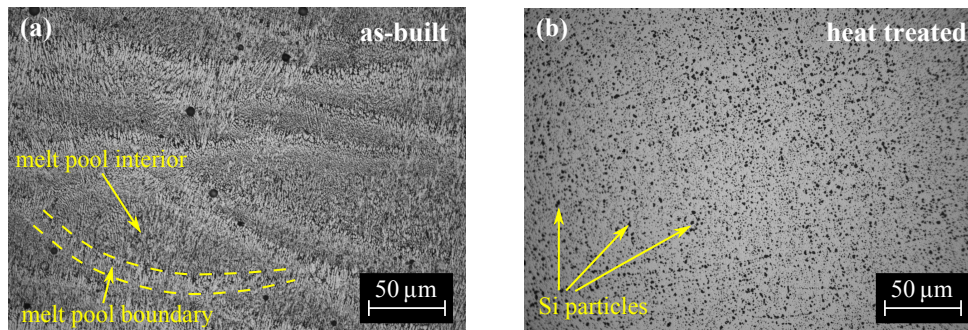

FIG. 3: Optical micrographs of SLM Al-Si10-Mg in its as-built (a) and heat treated (b) conditions.
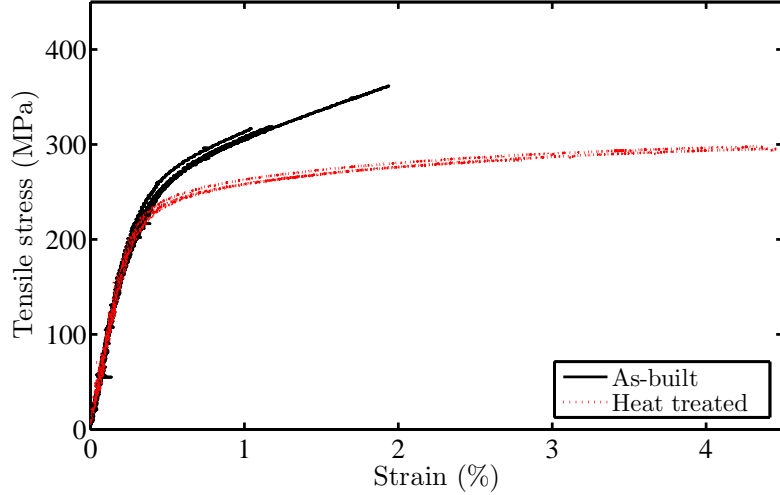
FIG. 4: Tensile stress-strain curves of as-built and heat treated SLM Al-Si10-Mg specimens.

that results from the SLM process, is transformed into a coarser-grained material, where the Si has agglomerated into particles with mean diameter just over 1 μm.

C.   Mechanical testing

Uniaxial static tension tests were conducted using an Instron 5581 universal testing machine equipped with a 50 kN load cell. The tests were conducted according to ASTM standard E8/E8M[28]. The load was applied at a displacement rate of 8.33×10^{-3} mm s^{-1}. A random white and black spatter pattern was applied to the tensile test specimens, allowing strain data to be collected using a video gauge. Three repeat tensile tests were made for the specimens in their as-built and heat treated conditions.

Room temperature fatigue tests were conducted using an Instron 8801 servo-hydraulic fatigue testing machine with a 100 kN load cell. A stress-controlled testing mode was used, following ASTM standard E466-07[29]. The cycling stress was sinusoidal with a frequency of 30 Hz, and a range of maximum stress, S_{max}, from 63 MPa to 220 MPa. The R value, equal to the ratio of minimum to maximum applied alternating stress, was 0.1. The runout limit was 3×10^7 cycles. Three repeat fatigue tests provided the data at each stress level.

III.   RESULTS AND DISCUSSION

The stress-strain curves from the static tension tests are presented in figure 4. There are two main noteworthy features. First, the ultimate strength of the material was reduced by $(12 \pm 3)\%$ from 330 ± 10 MPa to 292 ± 4 MPa after heat treatment , which is consistent with previous results concerning the effect of the heat treatment on the hardness[16] owing to the modified microstructure. Second, the ductility of the material was enhanced by the heat treatment. This is seen in the increase in strain-to-failure from $(1.4 \pm 0.3)\%$ to $(3.9 \pm 0.5)\%$, an increase by a factor of 2.8 ± 0.7.
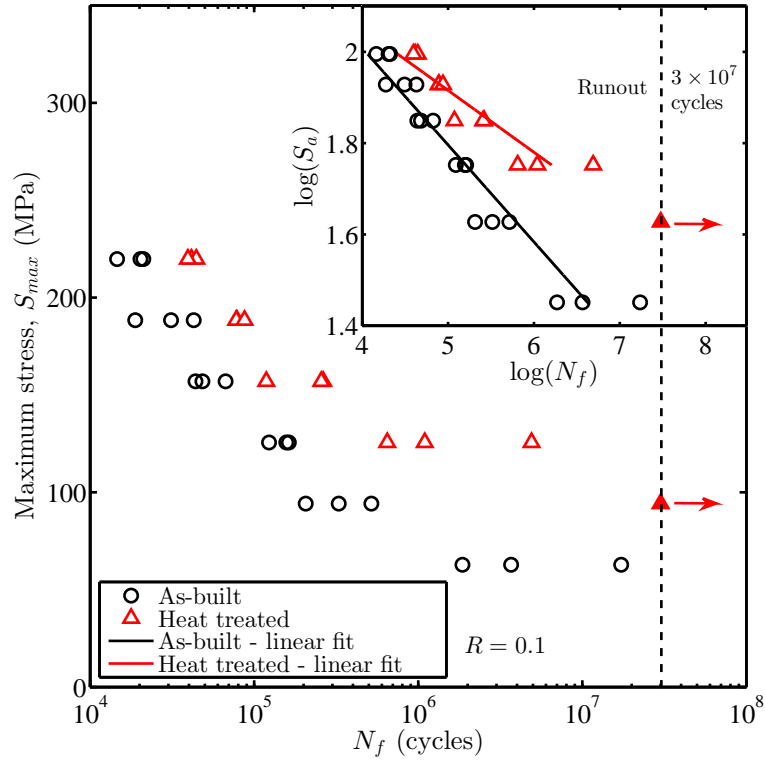
FIG. 5: S-N curves of as-built (black circles) and heat treated (red triangles) SLM Al-Si10-Mg specimens. A log-log plot is provided inset, along with corresponding linear fits.

Figure 5 provides fatigue curves of the as-built and heat treated material. At every level of applied maximum stress, S_{max}, the heat treated material survived a greater number of cycles before failure. The heat treatment also yielded a runout specimen, surviving 3×10^7 cycles, at a stress level of 94 MPa, while as-built specimens at the same stress had lifetimes of between just 2×10^5 and 5×10^5 cycles. The heat treatment, therefore, which increased the ductility of the SLM material by a factor of nearly three, also significantly improved its fatigue performance.

Brandl *et al.*[25] performed similar fatigue tests on SLM Al-Si10-Mg. The as-built and heat treated specimens of Brandl *et al.* had fatigue strengths of around 122 MPa and 170 MPa, respectively, at 10^6 cycles. Thus, those authors also reported enhanced fatigue strength brought about by heat treatment. The corresponding fatigue strengths in this work were lower, at 85 MPa and 134 MPa, respectively. However, in comparing these results, we must consider some important differences in the experimental procedures employed in the different studies. The most notable differences relate to the heat treatment and surface roughness of the examined specimens. The heat treatment of Brandl *et al.* consisted of a solution treatment for 6 hours at 525 °C, followed by water quenching and artificial ageing for 7 hours at 165 °C. See section II B for the heat treatment used here; the solution treatment duration was much shorter, at just 1 hour. According to Aboulkhair *et al.*[16], the solution treatment duration is likely to strongly affect the microstructure and hardness of the material, therefore will be like to affect the fatigue performance also. Secondly, the specimens of Brandl *et al.* were machined and polished

1021

	As-built	Heat treated
$\log(A)$	2.86 ± 0.09	2.6 ± 0.1
B	-0.21 ± 0.02	-0.14 ± 0.02

TABLE I: Fatigue curve fitting parameters for as-built and heat treated specimens.

in accordance with ASTM E466-07[29] (which specifies a maximum surface roughness of 2 μm), whereas the specimens in this work retained their as-built surface roughness. The surface roughness of SLM Al-Si10-Mg has previously been reported in the range of 12 μm[30] to 24 μm[31]. Since stress concentrations at the specimen surface cause crack initiation during cyclic loading, the reduced surface roughness of Brandl *et al.*'s specimens is likely to result in better fatigue performance than exhibited by the specimens examined here.

To provide more quantitative evidence regarding the fatigue performance of the as-built and heat treated material, numerical fitting was performed on the S-N data. A relationship of the form proposed by Basquin[32] was used, which can be expressed as[33],

$$S_a = A \ (N_f)^B, \tag{1}$$

where S_a is the stress amplitude, N_f is the number of cycles to failure, and A and B are constants. Taking base-ten logarithms provides

$$\log(S_a) = \log(A) + B \log(N_f). \tag{2}$$

The constant B is then the gradient of the S-N data when plotted on a log-log basis. This is provided in the inset of figure 5, which also includes the fit lines determined by linear regression. The fit parameters for the as-built and heat treated materials are provided in table I. The slope of the S-N log-log plot was reduced from -0.21 ± 0.02 to -0.14 ± 0.02, demonstrating the improvement in fatigue performance brought about by the heat treatment. Brandl *et al.* performed a different form of statistical analysis on their SLM Al-Si10-Mg fatigue data, so a direct comparison can not be made in this regard between our work and theirs. The best source for comparison is the work of Siddique *et al.*[22], who examined SLM Al-Si12 and also fitted their S-N fatigue data with a Basquin model. Their data yielded a log-log slope of -0.129, which agrees within error with that of our heat treated material. Agreement between our result and that of Siddique *et al.* was not expected, as the material composition and post-manufacture treatment were both different (again, their specimens were machined to lower the surface roughness), but it is encouraging that similar materials manufactured by the same process behave comparably. Siddique *et al.* also observed a fatigue strength at 10^6 cycles of approximately 80 MPa, which is very close to the 85 MPa seen for the as-built material here.

Other relevant results come from Buffière *et al.*[34], who studied the related alloy Al-Si7-Mg0.3 made by casting. They found values of B from -0.168 to -0.131 for a range of Al-Si7-Mg0.3 alloys with differing populations of pores. For the heat treated material studied here, the value of B is in the range obtained by Buffière *et al.*, indicating similarity of behaviour in our respective materials. This result is consistent with the similar chemical composition and microstructure of the two materials, i.e. an Al α phase interspersed with

Si particles. We must be cautious in drawing conclusions from this comparison, however, since the manufacturing processes are quite different, and the Si particles seen by Buffière *et al.* were larger than those seen here (3.1 μm cf. ∼ 1 μm in this work) and were less well dispersed throughout the material.

IV. CONCLUSIONS

We have shown that a heat treatment, of the kind which hardens and strengthens conventionally manufactured Al-Si alloys, results in reduced strength but significantly increased ductility and fatigue strength in SLM material. Brandl *et al.*[25] came to a similar conclusion regarding the effect of a heat treatment on the fatigue performance, and presented fatigue strengths which were in excess of those seen here for the same alloy. However, our specimens were tested with unmachined surfaces, so our results are more representative of the properties readily achievable by SLM without mechanical post-processing operations. These can be time consuming even for relatively simple geometries, and may often be impossible for the kind of complex lightweight parts, i.e. topology-optimised structures and lattices, that SLM is capable of producing. The results presented here, then, are novel and useful, and the information regarding the relationship of the microstructure and mechanical properties will aid the development of new heat treatments that maximise the desirable material properties with the minimum expenditure of effort and resources.

To expand upon this work, we will examine the effect of surface roughness of SLM parts on their fatigue performance. This will provide further insight into the respective importance of the microstructure and surface quality on the fatigue performance.

[1] Aremu, A. *et al. The effects of bidirectional evolutionary structural optimization parameters on an industrial designed component for additive manufacture.* P. I. Mech. Eng. B- J. Eng. 227, 794 (2013).

[2] Chahine, G. *et al. Application of Topology Optimization in Modern Additive Manufacturing.* In *Solid Freeform Fabrication Symposium*, 606–618 (2010).

[3] Brackett, D. *et al. Topology Optimization for Additive Manufacturing.* In *Solid Freeform Fabrication Symposium*, 348–362 (2011).

[4] Gardan, N. *Knowledge Management for Topological Optimization Integration in Additive Manufacturing.* Int. J. Manuf. Eng. 2014 (2014).

[5] Maskery, I. *et al. Mechanical Properties of Ti-6Al-4V Selectively Laser Melted Parts with Body-Centred-Cubic Lattices of Varying Cell Size.* Exp, Mech. 1–12 (2015).

[6] Brackett, D. *et al. An error diffusion based method to generate functionally graded cellular structures.* Comput. Struct. 138, 102 (2014).

[7] Brennan-Craddock, J. *et al. The design of impact absorbing structures for additive manufacture.* J. Phys.: Conference Series 382, 012042 (2012).

[8] Yan, C. *et al. Advanced lightweight 316L stainless steel cellular lattice structures fabricated via selective laser melting.* Mater. Design 55, 533 (2014).

[9] Yan, C. *et al. Evaluation of light-weight AlSi10Mg periodic cellular latticestructures fabricated via direct metal laser sintering.* J. Mater. Process Tech. 214, 856 (2014).

[10] Ushijima, K. *et al. An investigation into the compressive properties of stainless steel microlattice structures.* J. Sandw. Struct. Mat. 13, 303 (2011).

[11] Gorny, B. *et al. In situ characterization of the deformation and failure behavior of non-stochastic porous structures processed by selective laser melting.* Mat. Sci. and Eng.: A 528, 7962 (2011).

[12] Kooistra, G.W. *et al. Compressive behavior of age hardenable tetrahedral lattice truss structures made from aluminium.* Acta Mater. 52, 4229 (2004).

[13] Fleck, N.A. *et al. Micro-architectured materials: past, present and future.* Proc. R. Soc. A 466, 2495 (2010).

[14] Kempen, K. *et al. Mechanical Properties of AlSi10Mg Produced by Selective Laser Melting.* Physics Procedia 39, 439 (2012).

[15] Thijs, L. *et al. Fine-structured aluminium products with controllable texture by selective laser melting of pre-alloyed AlSi10Mg powder.* Acta Mater. 61, 1809 (2013).

[16] Aboulkhair, N. *et al. On the Precipitation Hardening of Selective Laser Melted AlSi10Mg.* Metall. Mater. Trans. A 1–5 (2015).

[17] Vandenbroucke, B. and Kruth, J.P. *Selective laser melting of biocompatible metals for rapid manufacturing of medical parts.* Rapid Prototyping Journal 13, 196 (2007).

[18] Vrancken, B. *et al. Heat treatment of Ti6Al4V produced by Selective Laser Melting: Microstructure and mechanical properties.* J. Alloy. Compd. 541, 177 (2012).

[19] Facchini, L. *et al. Ductility of a Ti-6Al-4V alloy produced by selective laser melting of prealloyed powders.* Rapid Prototyping Journal 16, 450 (2010).

[20] Dadbakhsh, S. *et al. Effect of selective laser melting layout on the quality of stainless steel parts.* Rapid Prototyping Journal 18, 241 (2012).

[21] Rafi, H. *et al. Microstructures and Mechanical Properties of Ti6Al4V Parts Fabricated by Selective Laser Melting and Electron Beam Melting.* J. Mater. Eng. Perform. 22, 3872 (2013).

[22] Siddique, S. *et al. Influence of process-induced microstructure and imperfections on mechanical properties of AlSi12 processed by selective laser melting.* J. Mater. Process Tech. 221, 205 (2015).

[23] Riemer, A. *et al. On the fatigue crack growth behavior in 316L stainless steel manufactured by selective laser melting.* Eng. Fract. Mech. 120, 15 (2014).

[24] Kanagarajah, P. *et al. Inconel 939 processed by selective laser melting: Effect of microstructure and temperature on the mechanical properties under static and cyclic loading.* Mat. Sci. and Eng.: A 588, 188 (2013).

[25] Brandl, E. *et al. Additive manufactured AlSi10Mg samples using Selective Laser Melting (SLM): Microstructure, high cycle fatigue, and fracture behavior.* Mater. Design 34, 159 (2012).

[26] Edwards, P. and Ramulu, M. *Fatigue performance evaluation of selective laser melted Ti-6Al-4V.* Mat. Sci. and Eng.: A 598, 327 (2014).

[27] Spierings, A. *et al. Fatigue performance of additive manufactured metallic parts.* Rapid Prototyping Journal 19, 88 (2013).

[28] *E8/E8M - 15. Standard Test Methods for Tension Testing of Metallic Materials.* ASTM

International (2015).

[29] *E466 - 07. Standard Practice for Conducting Force Controlled Constant Amplitude Axial Fatigue Tests of Metallic Materials.* ASTM International (2007).

[30] Liu, A. *et al. Properties of Test Coupons Fabricated by Selective Laser Melti.* Key Eng. mat. 447, 780 (2010).

[31] Calignano, F. *et al. Influence of process parameters on surface roughness of aluminum parts produced by DMLS.* Int. J. Adv. Manuf. Technol. 67, 2743 (2013).

[32] Basquin, O. *The Exponential Law of Endurance Tests.* Proc. ASTM, part II 10 (1910).

[33] Stephens, R. *et al. Metal Fatigue in Engineering.* Wiley (2001).

[34] Buffière, J.Y. *et al. Experimental study of porosity and its relation to fatigue mechanisms of model Al-Si7-Mg0.3 cast Al alloys.* Mat. Sci. and Eng.: A 316, 115 (2001).